Calibration Faint Stars Needs for RVS

RVS Calibration

prepared by: C. Allende Prieto, M. Cropper
approved by:

reference: GAIA-C6-SP-MSSL-CAP-006
issue: 1
revision: 3
date: November 27, 2009
status:

Abstract

Optical distortions across the focal plane make the shape of the point spread function vary with CCD, wavelength, and across-scan position. Charge transfer inefficiency in the serial register will enhanced the variations in the across-scan direction and introduce an additional dependence with source brightness. Tracking these variations for RVS spectra of targets fainter than $G_{\rm rvs} = 7$ mag requires *calibration faint stars*: objects that are fainter and therefore would nominally have one dimensional windows assigned, but which are given two dimensional windows for calibration purposes. We examine how these objects can be used for RVS calibration and suggest modifications to the selection scheme proposed in GAIA-C3-TN-ZAH-MB-025: the fraction of CFS is capped to 10% per 2-magnitude bin at $G < 14$ and increased from that proposal to 5–10% in the magnitude bin $15 < G < 17$. We also suggest ways in which the impact on the telemetry volume can be minimized.

Document History

Issue	Revision	Date	Author	Comment
1	1	2009-11-24	CAP	Draft
1	2	2009-11-25	MSC	Edited
1	3	2009-11-27	CAP	Edited

Contents

1 Introduction

An accurate knowledge of the AC line spread function (LSF), which we will represent by $P(x)$ and satisfies $\int P(x)dx = 1$, is necessary for separating the flux contributions of sources that overlap (*deblending*), as well as to correct for possible charge losses outside of the assigned RVS windows and other radiation effects: an example might be a correct evaluation of the CTI effects in the AL direction. The LSF shape can be directly studied from class 0 windows: 2D windows available for sources with $G_{\rm rvs} < 7$. At fainter magnitudes, our ability to constrain the LSF shape relies of calibration faint stars (CFS), 2D windows used for calibration purposes on a fraction of the sources, and in particular on being able to accumulate enough signal by adding an appropriate number of them at all magnitudes.

Charge transfer inefficiency (CTI) in the serial register will enhance the expected AC LSF variations along the AC direction, and produce leakage of charge out of the CCD windows. Dealing with these issues requires a finely tuned selection strategy for CFS, ensuring that the LSF in the across-scan direction can be characterized properly.

2 AC Line Spread Function Characterization

The $G_{\rm rvs}$ magnitude and the total signal that a source's transit produces on an RVS CCD (S, in electrons) are related by

$$G_{\rm rvs} \simeq -2.5 \log_{10} S + 22.5866 \quad \text{mag} \tag{1}$$

(see GAIA-C6-SP-MSSL-CAP-003). At any given AL position of 1260 in the window, the total signal is

$$I = \int I(x)dx = \frac{1}{1260} \times 10^{(22.5866-G_{\rm rvs})/2.5} \simeq 859545 \times 10^{-Grvs/2.5} \quad \text{e}^-, \tag{2}$$

and we will approximate the associated uncertainty (class 0 windows) as

$$\sigma_I \simeq \sqrt{I + 10\sigma_0^2} \quad \text{e}^-, \tag{3}$$

where σ_0 is the readout noise, approximately 4.6 e$^-$.

The signal spreads in AC according to the line spread function, which for our purposes will include optical, discretization (sampling), and CTI effects, i.e. it is a function of wavelength, AC position, and the brightness of the source[1]. The signal variation in AC is therefore $I \times P(x)$,

[1] Note that it may not be desirable to have an LSF that depends on brightness, and the effects that make the image of a source point to depend on the signal level can be effectively decoupled from the LSF by defining the latter appropriately. Nevertheless, for convenience, we will use a relaxed language in this document, referring to the LSF as the effective response of the system to a source point, which due to CTI in the serial register will depend on magnitude. We refer the reader to GAIA-C3-TN-LU-LL-080 and references therein for more details on the proposed LSF definition for Gaia.

where $0 < x < 10$ for the RVS windows. In the calibrations, the variations of the LSF with wavelength will be explored by analyzing a number (N) of spectral segments; we will refer to these as *chunks*. The signal will be summed over all AL samples in a *chunk* before analyzing the shape of the AC LSF, so the signal in one of AC profiles to examine is

$$I(x) = \frac{1260}{N} \times 859545 \times 10^{-Grvs/2.5} \times P(x) \quad e^{-}. \tag{4}$$

We want to find out how much signal is needed to constrain the LSF parameters to a certain level of precision. We choose that level by performing montecarlo simulations and fitting a functional LSF form to them. For example, for a Gaussian LSF characterized by a width σ, the expected signal for a spectrum centered at $x = c$ is

$$I(x) \simeq \frac{859545}{\sqrt{2\pi}\sigma} \exp\left(\frac{-2\ln 10\sigma^2 G_{\rm rvs} - 2.5(x-c)^2}{5\sigma^2}\right), \tag{5}$$

and, assuming an ideal performance of the Video Processing Unit (VPU), where the values of c for different sources should be uniformly distributed in the range $4.5 < c < 5.5$, *i.e.* within 1/2 pixel of the window center. Analyzing simulations of sources with different brightnesses we find that the LSF width can be derived for ten wavelength bins with a precision of about 1 % from a single observation of a source with $G_{\rm rvs} = 8.8$, and 2% from a source with $G_{\rm rvs} = 9.8$ (see Fig. 1)[2].

Achieving an equivalent signal-to-noise at fainter magnitudes will require adding data from transits of different objects. The combination of multiple observations can potentially alter the profiles by introducing additional broadening, but this effect should be modest given the expected accuracy of the window centers. With an assumed LSF FWHM of about 3 pixels, fitting profiles with a low signal-to-noise ratio is challenging, and as Fig. 1 illustrates, it is possible to improve precision by resampling the AC profiles with a finer wavelength step, splitting the sample of calibrators into several groups .

A Gaussian profile corresponds to an oversimplified LSF. Realistic profiles can only be represented by more complex shapes, involving a larger number of parameters, and a similar level of precision will demand higher signal-to-noise levels. In what follows we shall make the assumption that characterizing the AC LSF shape satisfactorily requires a signal-to-noise ratio equivalent to a single observation of a $G_{\rm rvs} = 9$ star. This assumption **must** be checked against more detailed simulations from CU2 in the future.

[2] We similarly derive that errors in the determination of the central location are 1 % and 2% for observations with $G_{\rm rvs} = 9.1$ and 10.1 mag, respectively

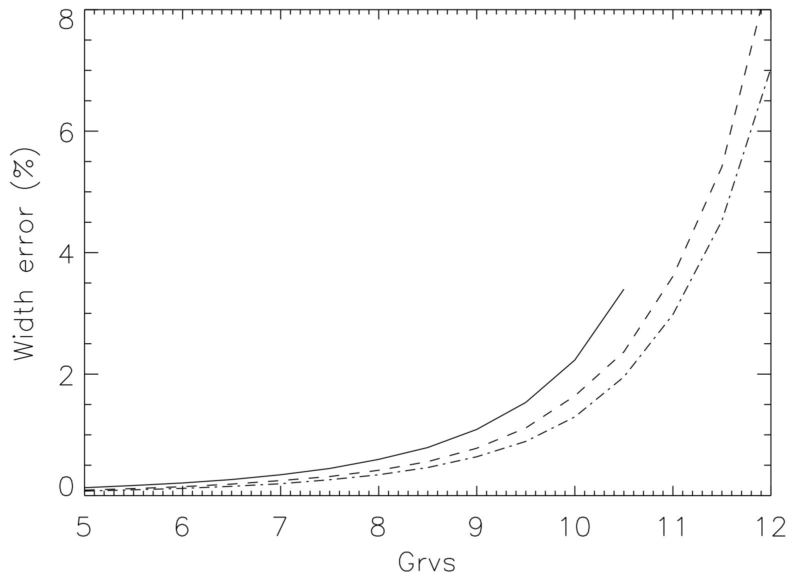

Figure 1: Uncertainty in the determination of the width of a Gaussian LSF from observations of sources with different brightness. The signal in the simulated profiles has been collapsed in AL into ten different bins (*chunks*). The assumed LSF FWHM is 3 pixels. Using sub-pixel sampling improves performance. The solid line shows the nominal result without resampling. The broken line corresponds to having 2 data points per AC pixel and the dash-dotted line to having 3 data points per AC pixel.

3 Adding up faint calibration stars

We are interested in calculating how many CFS of a given magnitude G are needed in order to achieve the signal-to-noise equivalent to a single observation of a $G_0 = 9$ star. In this exercise we will ignore the fact that the LSF shape varies with magnitude.

After collapsing a spectrum in AC, the average signal-to-noise ratio in AL at any given magnitude can be derived from Eqs. 2 and 3. Defining $\alpha = 859545$ and $\beta = 10 \times \sigma_0^2 = 211.6$, that is

$$\frac{I}{\sigma_I} = \frac{\alpha \times 10^{-2G/5}}{\sqrt{\alpha \times 10^{-2G/5} + \beta}}. \tag{6}$$

The signal-to-noise for the addition of n spectra is $\sqrt{n} \times I/\sigma_I$, and by equating the signal-to-noise for a single spectrum with a magnitude G_0 to that from the combination of n spectra with a magnitude G, we find that

$$n = 10^{\frac{4}{5}(G-G_0)} \quad \frac{\alpha \times 10^{-2G/5} + \beta}{\alpha \times 10^{-2G_0/5} + \beta}. \tag{7}$$

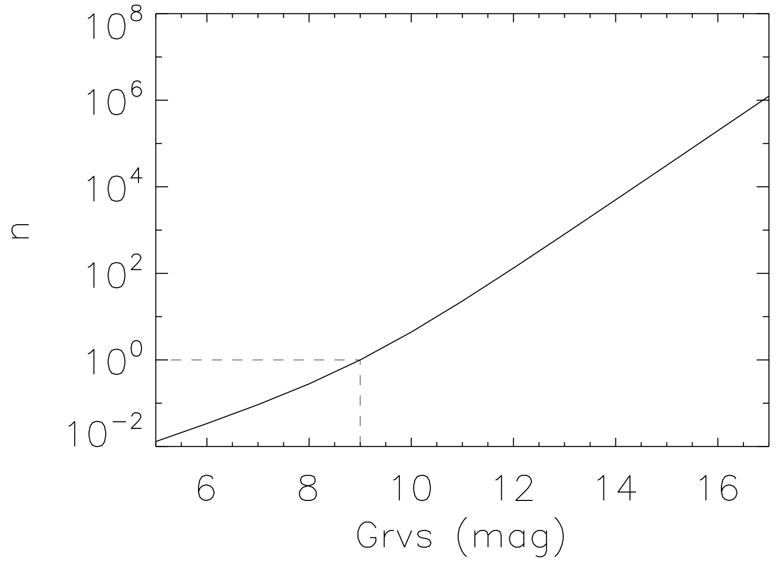

Figure 2: Number of faint stars needed to achieve a total signal-to-noise ratio per collapsed AL sample equivalent to a single observation with $G_{\rm rvs} = 9$. See Eq. 7.

Eq. 7 for $G_0 = 9$ gives the result shown in Figure 2. Several million stars must be co-added at the faint end in order to build up the equivalent of an eighth magnitude calibrator.

4 CFS statistics

To estimate the number of stars observed by the RVS CCDs, we will approximate the total number of stars observed in the $G_{\rm rvs}$ band in the sky by

$$\log N_G \simeq \gamma + 0.18 \times G_{\rm rvs}, \tag{8}$$

(see GAIA-C6-SP-MSSL-CAP-002), which is a reasonable approximation between $12 < G < 20$ mag, and determine γ by requiring that the total observed by RVS, approximately in the band $5 < G_{\rm rvs} < 17$ are

$$\int_{G=5}^{G=17} N_G \ dG = \frac{10^\gamma}{0.18 \ln 10} \left(10^{0.18\times17} - 10^{0.18\times5}\right) = 10^8, \tag{9}$$

which leads to $\gamma \simeq 4.56$.

On average, any star will be observed about 40 times by RVS, and therefore the number of observations will be approximately $40 \times N_G$. On the other hand, the AC LSF calibration should be performed independently for each CCD, and each CCD row will only see one fourth of

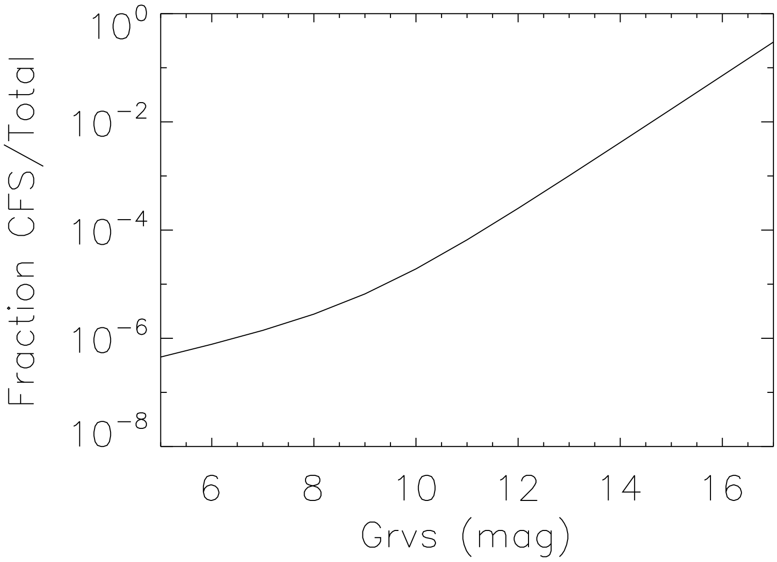

Figure 3: Fraction of all observations needed to determine the shape of the AC LSF with the same accuracy that would be obtained from a single $G_{\rm rvs} \sim 9$ mag observation. See §4 for details of the assumptions involved.

the transits. Additional factors need to be considered, as mapping the LSF variations with AC on any given detector will require an analysis of a number of zones, which we will take as 10 for now. These three factors approximately cancel each other, but we still will need to resolve variations of the LSF periodically with time, perhaps every semester or 10 times during the mission[3]. By multiplying Equation 7 by $10/N_G$ we can estimate the total number of CFS needed. This is illustrated in Fig. 3. At around 13 magnitude, about 0.1% of observations are needed to become a CFS, while the fraction reaches nearly 1.7% at $G_{\rm rvs} = 15$.

5 CFS proposal

By breaking the magnitude range of the CFS into 2–magnitude bins, the estimates from the previous section can be translated into the numbers in Table 1. These figures are for 10 independent *calibration units* during the mission lifetime.

The minimum number of CFS required for RVS AC LSF calibration at magnitudes fainter than $G_{\rm rvs} \sim 13$ is very small, and other factors will drive the demand for CFS in that range. On the other hand, it is in that magnitude range where the RVS spectra provide the most astrophys-

[3]This period does not preclude us from evaluate the LSF more frequently using running time windows for the CFS samples.

Table 1: Number of observations available for one of 10 AC zones in any given CCD and in each magnitude range (roughly equivalent to the number of stars in the sky within that magnitude range), and how many would be needed to become CFS in order to have the equivalent quality of a single observation at $G_{\rm rvs} \simeq 9$ every six months. Note that our *universe model*, *i.e.* Eq. 8, is limited to $G_{\rm rvs} > 12$, and the number of observations available for brighter stars is seriously overestimated.

$G_{\rm rvs}$ range (mag)	Number of CFS ($10 \times n$)	Observations Available	Fraction (%)
7.0 – 9.0	7.34e+00	2.06e+06	0.0004
9.0 –11.0	1.35e+02	4.71e+06	0.0029
11.0 –13.0	4.35e+03	1.08e+07	0.0403
13.0 –15.0	1.67e+05	2.47e+07	0.6731
15.0 –17.0	6.59e+06	5.67e+07	11.624

ically important information: surface temperatures, gravities, and chemical compositions. It is therefore important for RVS that the maximum data quality be maintain in this range. The readout noise in a class-0 window sample is 30-times higher than in a class-2 window normally used for this brightness, and a significant fraction of CFS will lead to a serious degradation of the overall RVS performance.

Accumulating the necessary signal at the faint end will be hard. Our rough estimate points to a fraction of stars as high as 10 %, but the increased telemetry volume will require to keep that fraction as low as possible, perhaps at a 5% level.

We therefore propose that not more than 10% of the observations in the magnitude bins at $G < 14$ are acquired as CFS, and that a similar or slightly lower level be maintained at the faint end of the RVS magnitude range ($15 < G < 17$). Attending to the needs described in GAIA-C3-TN-ZAH-MB-025, and without regard to the telemetry limits, to be examined in more detail later, we propose to acquire as CFS the following fractions:

- 3 % of all measurements of sources with $7 < G \leq 10$
- 10% of all measurements of sources with $11 < G \leq 11.5$
- 10% of all measurements of sources with $11.5 < G \leq 13$
- 10% of all measurements of sources with $13 < G \leq 14$
- 1% of all measurements of sources with $14 < G \leq 15$
- 5–10% of all measurements of sources with $15 < G \leq 17$
- 0.3% of all measurements of sources with $17 < G \leq 20$.

This proposal could double the RVS telemetry volume. We therefore suggest that RVS CFS windows respect the transition between HR and LR at $G_{\rm rvs} = 10$. We further note that, should it be possible, a greater level of on-chip binning in the along-scan direction, up to the length of the wavelength chunks for LSF calibration (100–300 AL samples), would help significantly to reduce the data volume and achieve higher signal-to-noise ratios with fewer CFS on the faint end. In the RVS case, due to the increased readout noise, faint CFS ($15 < G < 17$) will not provide enough signal-to-noise ratio to measure radial velocities.